

Remarks concerning the Inner Detector material budget

Allan G. Clark and Alan Poppleton

Abstract

The material budget of the ATLAS Inner Detector is described using a simplified detector geometry. A specification of $0.2X_0$ is proposed for the integrated material to the last discrete tracker measurement. The pixel detector and associated services are identified as one important (excessive) contribution to the material. A revised pixel layout with a new pixel routing is suggested. Significant items requiring further study are noted. Very preliminary suggestions relevant to other sub-detectors are made.

1.0 Introduction

There has been considerable recent activity [1-3] to insert in the ATLAS simulation realistic service material and routing on the basis of the post-Morges Inner Detector layout. Using numbers supplied to the DICE Monte Carlo, T. Pal [1] has measured an integrated material budget reaching $\sim 0.35X_0$ at the entrance to the TRT with a total exceeding $1X_0$ in front of the cryostat. This material distribution is shown in Figure 1.

Features which are of concern for robust tracking (especially electron identification) include

- a rapid increase in material beyond $|\eta|=0.6$,
- a maximum of the SCT/pixel material traversed which is not well matched to the region of services in the calorimeters.

A simple description of the tracker and services is used to represent the existing layout. A comparison with the services input to DICE is described in Section 2. Realistic ways to reduce the material budget in the SCT and pixels, within the envelope provided at present by the TRT, are investigated. This has resulted in a revised pixel layout and service routing, which is described in Section 3. In Section 4, we note some consequences and raise some questions concerning this revised layout: performance for the tracker and the detector as a whole, mechanical feasibility, and fiscal/organizational constraints.

No detailed tuning of the layout has been considered in this note; for example, a detailed optimization of tracker radii to maintain coverage near (evolving) service cracks is not

attempted. Similarly, the engineering study to reduce module or support material is not addressed. That study is obviously essential.

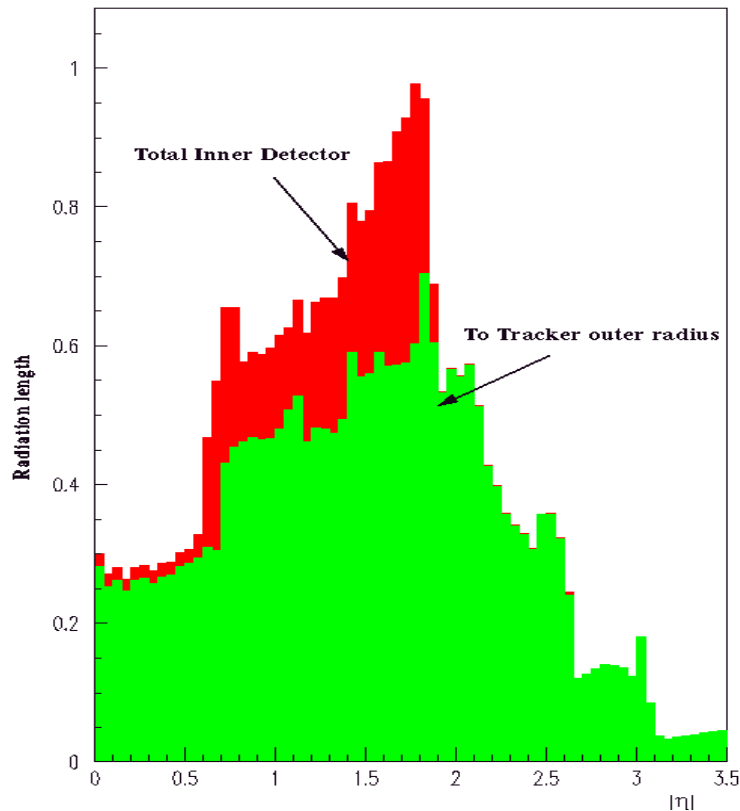


Figure 1: Inner detector material (in radiation lengths) excluding patch panels. The total amount and the integral to the last track measurement are shown.

Included in the tracking performance criteria of Ref.[4] are a minimum of 6 semiconductor track layers to ensure at least 5 measured space points. Given that no other space point track measurements are available, and that this is an absolute minimum to enable track reconstruction from the discrete layers, the requirement is maintained.

The requirement of Ref.[4] on electron identification and reconstruction is a 90% track efficiency for isolated electrons. Ref.[5] uses the IPATREC package to reconstruct isolated $p_T=20$ GeV/c electrons with the “Cosener’s House” layout; the total material assumed for that layout in the range $|\eta|<0.7$ is $0.25X_0$, with $<0.2X_0$ to the sixth semiconductor layer. The global track efficiency after bremsstrahlung recovery is $\epsilon=0.92$ ($\epsilon=0.88$ after pile-up), but falls to $\epsilon=0.81$ (respectively $\epsilon=0.77$) in the range $0.7<|\eta|<1.4$ where the material varies between $0.3X_0$ and $0.6X_0$. Prior to bremsstrahlung recovery [6], as relevant for a less isolated environment, the track reconstruction efficiency is $\epsilon=0.81$ in the region $0.0<|\eta|<0.7$. We infer that a target specification of $0.2X_0$ at the entrance to the TRT should certainly not be exceeded.

It is noted in passing that the optimal matching for extrapolations between the continuous and discrete subdetectors is not specified by Ref.[4].

2.0 Material in the existing layout

The existing layout is shown in Figure 2, together with service routings. Tables 1 and 2 list the assumed module and service material. Services marked 'radial' are reduced in thickness as a function of the radius. Services transferred inward therefore have an increased material contribution.

In addition to the material quoted, patch panels of $0.11-0.13 X_0$ exist at a radius $1.08 < r < 1.15\text{m}$ (in front of the cryostat), for $0.6 < z < 1.0\text{m}$. These patch panels have not been included in our material estimates, nor have they been included in Figure 1.

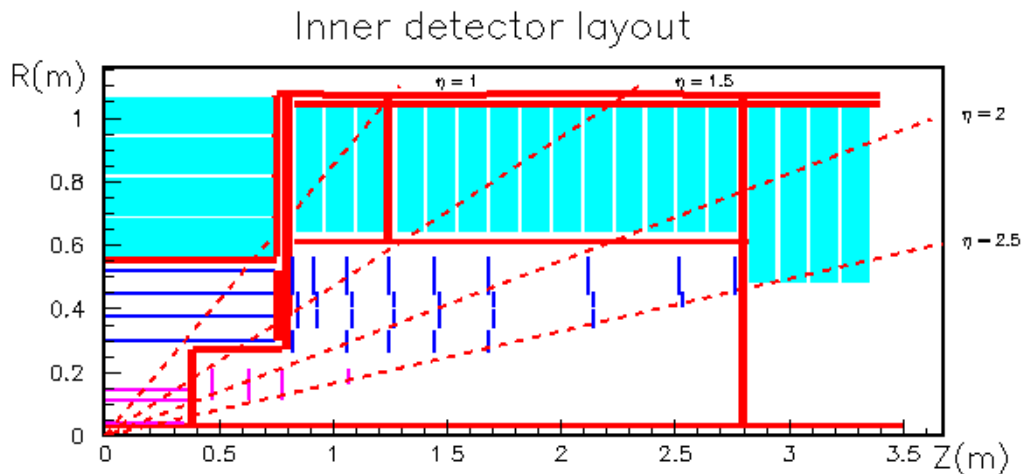


Figure 2: Schematic inner detector with service routing

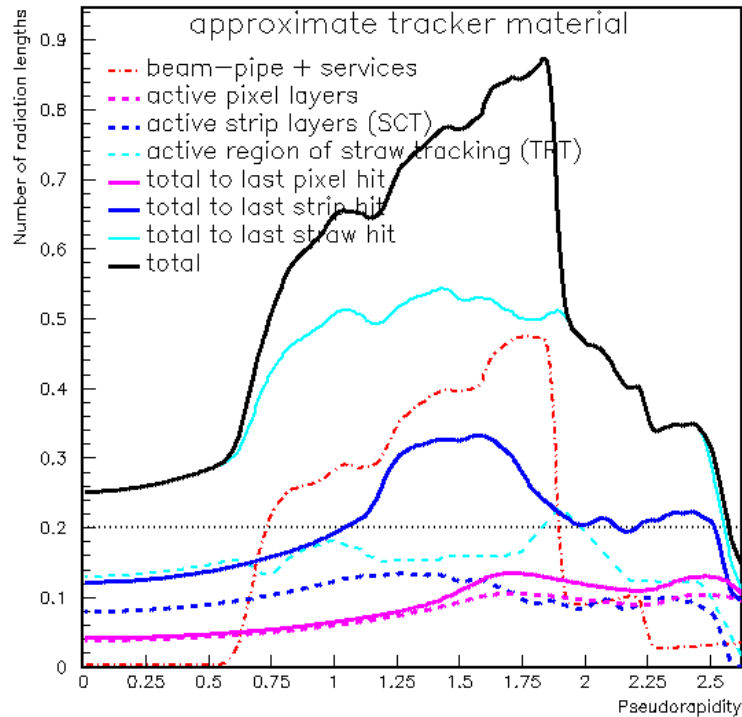


Figure 3: Evaluated material distribution as a function of $|\eta|$ for the base-line layout assuming the values quoted in Tables 1 and 2

Small differences between Figures 1 and 2 are explained by the radial dependence of services, and by vertex smearing, in Figure 2.

Table 1: Active material input assumed for SCT, pixels.

Object	Layer	z or 1/2 length(m)	radius(m)	X ₀	X ₀ service
SCT	Layer 1-4	0.74	0.30-0.52	0.02	0.0092 radial
	Ring 1-9	various z	0.26-0.56	0.02	0.015 @ r=.62 including TRT support
Pixel	Layer b	0.35	0.04	0.013	0.0135 radial
	1-2	0.387	0.11, 0.142	0.013	0.0137 radial
	Ring 1-4	0.473,0.635, 0.776, 1.072	0.11-0.208, 0.15-0.208 ring 4	0.0115	none
Beam	-	-	0.03	0.003	-

Table 2. TRT and inert material

Object	Comment	Position r(m)	Position z (m)	Material X ₀
TRT	Barrel support	0.55	0.0-0.74	0.015
	Layers 1-4	0.56-1.03	0.0-0.74	0.029
	Services	0.56-10.3	0.76	0.07
	Services	1.07	0.76-0.96	0.01
	Services (SCT barrel)	1.07	0.76-0.96	0.0145
Forward TRT	Active layers	0.64-1.03	Full density Various z	0.0240
	Active layers	0.64-1.03	'Extra' density Various z	0.03
	Active layers	0.64-1.03	Half density Various z	0.0120
TRT	Forward support & electronics	1.03-1.06	0.83-3.38	0.050
TRT	Services	1.07	0.96-1.68	0.018
	Services	1.07	1.68-2.54	0.030
	Services	1.07	2.54-3.40	0.038
SCT	Barrel flange	0.30-0.52	0.76	0.015
	Services	1.07	0.96-1.68	0.019
	Services	1.07	1.68-2.54	0.0235
	Services	1.07	2.54-3.40	0.028
	Services	0.56-1.03	1.67 2.80	0.030 radial 0.015 radial

The material distribution for the layout of Figure 2 is shown in Figure 3. Of crucial importance for pattern recognition is the minimisation of material internal to the continuous track-

ing layers (TRT). In the layout of Figure 2, a total material of $0.30\text{-}0.34X_0$ exists in the range $1.2 < |\eta| < 1.7$.

The material distribution is not well matched to the reduced calorimeter performance in the range $1.4 < |\eta| < 1.8$, it would be helpful to attempt to push the services into that region, or beyond into the end-cap region $|\eta| > 2$.

In the case of high-luminosity operation, it is official Atlas strategy to remove the b-layer. The material has been evaluated for this case, by removing both the b-layer and its associated services. Figure 4 shows the resulting distribution in $|\eta|$ of the material; a maximum of $0.29X_0$ is estimated

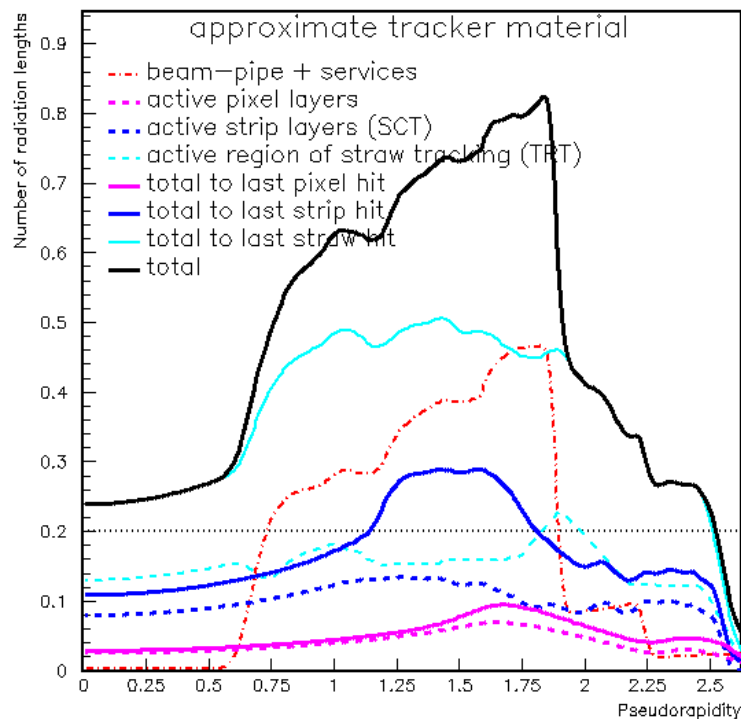


Figure 4: As for Figure 3 after removal of the pixel b-layer and associated services

For completeness, Figures 5 and 6 show the mean number of discrete space points as a function of $|\eta|$, with and without the b-layer. The following comments are appropriate:

- ‘Dog leg’ services are dangerous, in the sense that tracks can cross the same services several times in a restricted $|\eta|$ range. This is the case for the barrel pixel services in particular, for the existing design. It is also the case for the other services passing the tracking crack between the barrel and forward regions.

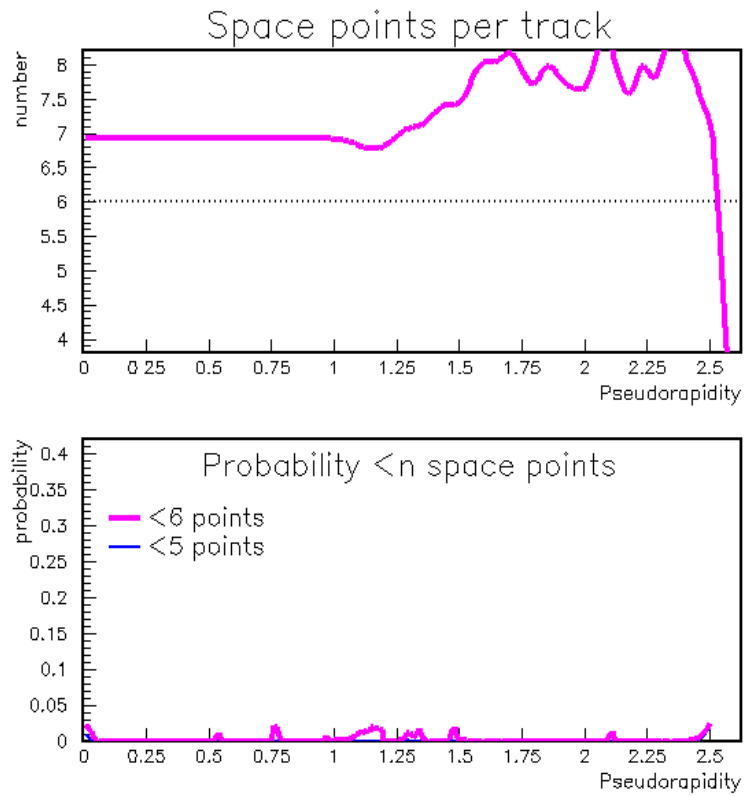


Figure 5: Mean number of space points per track versus $|\eta|$ for the base-line layout assuming full efficiency.

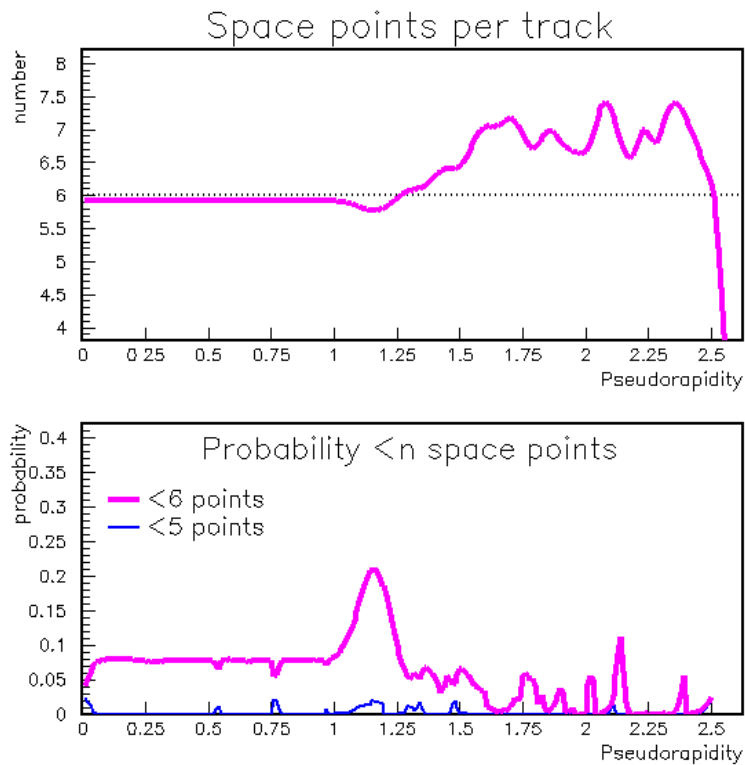


Figure 6: As above excluding the pixel b-layer.

- When traversing material, incident angle effects can become important; the quoted numbers illustrate this effect.

$$|\eta|=1.0 \quad \theta=40.4^\circ \quad 1/\sin(\theta)=1.54$$

$$|\eta|=1.5 \quad \theta=25.2^\circ \quad 1/\sin(\theta)=2.35$$

$$|\eta|=2.0 \quad \theta=15.4^\circ \quad 1/\sin(\theta)=3.76$$

$$|\eta|=2.5 \quad \theta=9.39^\circ \quad 1/\sin(\theta)=6.13$$

Given this angle effect, it is difficult in the existing layout to reduce the material from the active layers alone to less than $\sim 0.2 X_0$.

- No account is taken of the forward pixel services, or of the forward pixel supports, in the distributions of Figures 2 through 6. This results in an underestimate of the tracker material.

3.0 Changes to the pixel services, and a revised pixel layout

3.1 Pixel services

An initial attempt has been made to study a re-routing of the pixel services, for the existing layout, with the aim of removing the dog-leg of services preceding the SCT layers. The services from the $r=11\text{cm}$ and $r=14.2\text{cm}$ layers have been extended radially inward to the $r=4\text{cm}$ limit, and in addition services of $0.01X_0$ for 2 pixel wheels are assumed (the other 2 pixel wheels extend beyond the $|\eta|=2.5$ boundary). The negative radial impact of this service routing more than compensates the $1/\sin(\theta)$ effect of a routing parallel to the beam pipe in the case of a tracker covering $|\eta|<2.5$. For a tracker volume $|\eta|<2.0$, an alternative routing would be preferred. The resulting layout and estimated material distribution are shown in Figures 7 and 8.

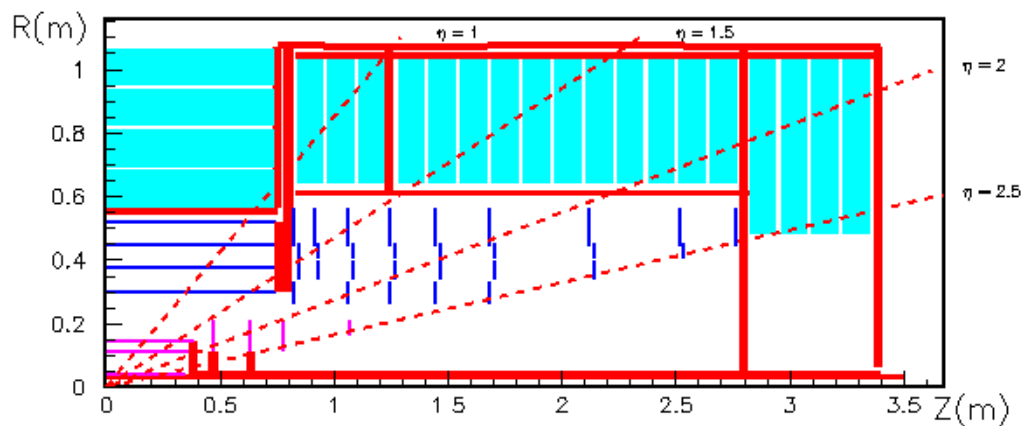


Figure 7: Base-line layout with re-routed pixel services

The effect of this re-routing is to *reduce* the maximum material to $0.26X_0$ in the range $|\eta|<2.0$, at the expense of an increased material budget in the region $|\eta|>2.0$, reaching $0.29X_0$.

The re-routing of services in this way requires justification on the following points:

- What emphasis does Atlas place on the relative tracking performances of the regions $|\eta| < 2.0$ and the region $2.0 < |\eta| < 2.5$?
- What is the influence of the material for relevant physics processes of the $E_T(\text{miss})$ resolution due to energy mismeasurement in the forward calorimeters, and what is the effect on detector operation of spurious hits in the forward discrete and continuous trackers (splash-back)?
- What is the radiation tolerance of cables extending in the forward direction? The total heat generation in the forward direction is estimated [8] to be $\sim 1.6\text{kW}$.

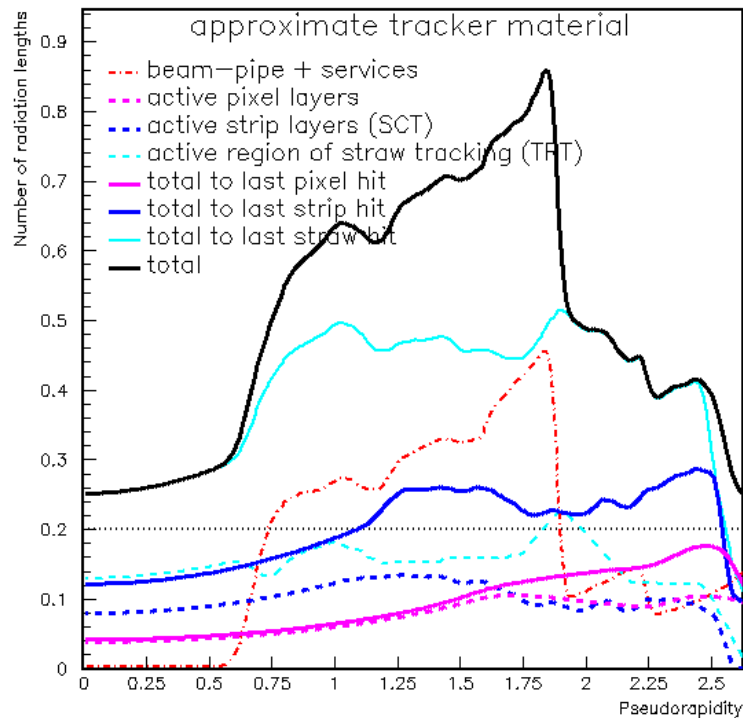


Figure 8: Material distribution for the layout of Figure 7.

3.2 A revised pixel layout

In an effort to further reduce the detector material, a revised pixel layout has been studied. Although the $r=4\text{cm}$ b-layer is for low-luminosity operation [4], it is widely regarded as desirable at high luminosity for b-tagging [7].

The proposed layout replaces the existing 3-layer pixel barrel by 2 extended barrel layers:

Layer 1:	Half-length 46cm	$ \eta =2.73$ for 1σ vertex offset	Radius 6cm
Layer 2	Half-length 46cm	$ \eta =2.14$ for 1σ vertex offset	Radius 11cm.

A pixel support of $0.003X_0$ extends at $R=11\text{cm}$ beyond the tracker acceptance. Two of the 4 pixel wheels have been removed, since the acceptance is covered by the longer barrel. This layout is *not* fully optimized; and future design iterations are expected, respecting:

- the minimisation of total material and service material within the acceptance (only one layer, the $r=11$ cm barrel, has services within the $|\eta|=2.5$ acceptance),
- an adherence to tracker specifications of [4] on the number (6) of discrete space points,
- acceptable b-tagging performance at high luminosity,
- mechanical feasibility.

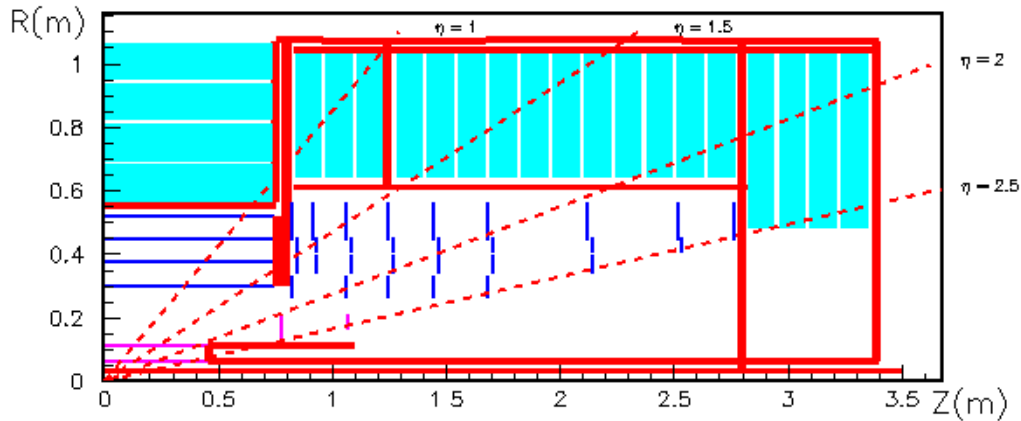


Figure 9: Revised pixel layout with 2 extended barrel layers.

Figure 9 shows the proposed tracker layout, and Figure 10 shows the estimated distribution of material as a function of $|\eta|$. Figure 11 shows the mean number of discrete hits in the new layout, as a function of $|\eta|$.

- The total material estimate (Figure 10) reaches $0.23X_0$, excepting the region $|\eta|>2.2$, where it reaches $0.26X_0$. This remains in excess of requirements. A further improvement depends on an improved SCT layout, and on detailed engineering optimisation.
- The impact parameter for b-tagging studies is deteriorated from $\sim(12+71/p_T)\mu\text{m}$ to $\sim(14+103/p_T)\mu\text{m}$ at 90° , and for both layouts this deteriorates in the forward direction. For a $0.01X_0$ layer, as assumed in the Technical Proposal (TP), the p_T -dependent constant becomes respectively $63\mu\text{m}$ and $93\mu\text{m}$. The numbers are larger than quoted in the TP or Ref. [7], because of the inclusion of a correct multiple scattering treatment.
- The hit distribution of Figure 11 compares favourably to that of the original high-luminosity layout (see Figure 6), despite the lack of wheel optimization.
- The total pixel area has been reduced

	Barrel (m^2)	Forward (m^2)	Total (m^2)	
Old	1.4	0.71	2.11	
New	0.98	0.31	1.30	<u>Ratio=0.62</u>

The 6cm barrel has a total area of 0.35 m^2 , to be compared with 0.18m^2 for the $r=4\text{cm}$ layer;

- If a 4cm radius b-layer is to be used for b-tagging at high luminosity, layer replacement is required on a regular basis. Table 3 below shows (inferred from [7]) the depletion voltage increased as calculated by the Hamburg group, during one full year of operation at high luminosity (10^7 secs at 10^{34} $\text{cm}^{-2}\text{sec}^{-1}$)

R (cm)	$ \eta $	V_D [V]	Fluence ($\times 10^{14} \text{cm}^{-2}$)	R (cm)	$ \eta $	V_D [V]	Fluence ($\times 10^{14} \text{cm}^{-2}$)
4.	0.	130	3.7	6	0.	80	1.8
					2.2	130	3.6
	2.5	510	8.1		2.5	~ 160	4.0
	2.9	590	8.9				

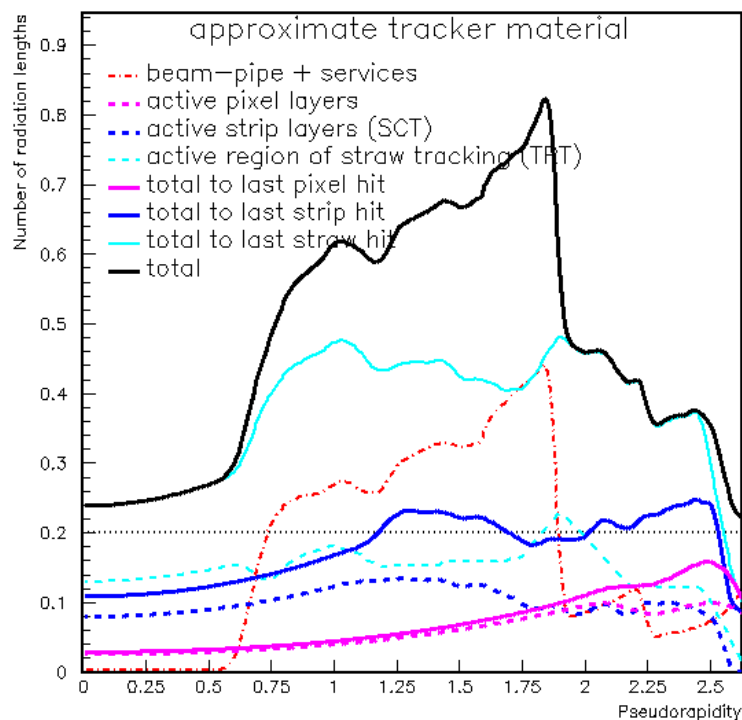


Figure 10: Material distribution for the layout of Figure 9.

It is obvious that if such a layout with an $r=6\text{cm}$ layer is chosen, *or* if the $r=4\text{cm}$ layer is foreseen at high luminosity, frequent replacement is required, as already noted. This layout improves the robustness of b-tagging, given the above assumptions. Such a layout is *not* feasible unless Atlas has a replacement strategy, involving the commitment of one or more national laboratory and a relevant financial profile.

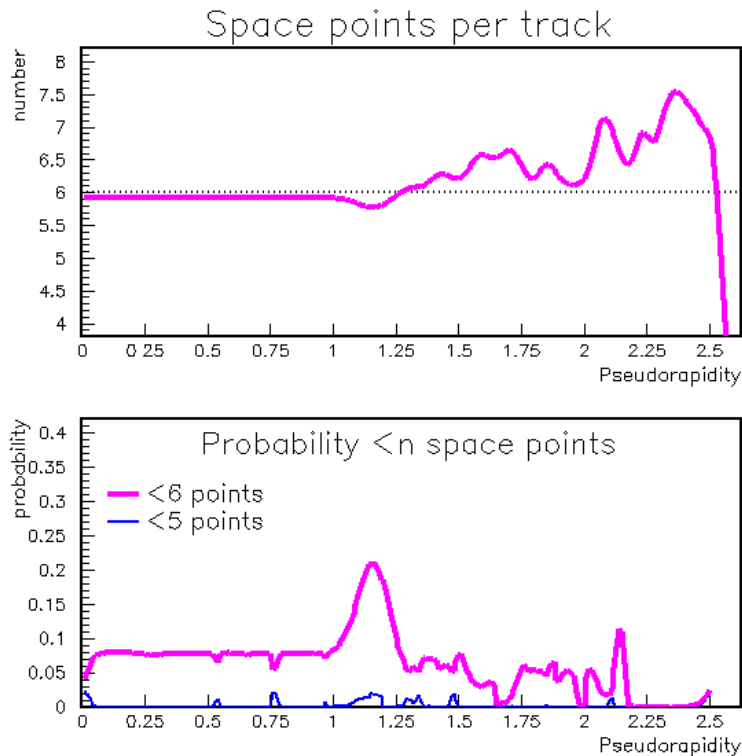


Figure 11: Mean number of space points per track versus $|\eta|$ for layout of Figure 9.

3.3 Material due to SCT/pixel services external to the SCT/pixel envelope

On the basis of the proposed layout shown in Figure 9, the contribution of SCT and pixel services external to the SCT, but within the cryostat is evaluated. Again, patch panels are not included. Figure 12 compares the total material with Figure 10, after the removal of all SCT services (barrel and wheel) passing through cracks of the TRT, and services external to the TRT. The SCT service and support material is estimated to be $\sim 0.02X_0$ to the last straw tube, and $\sim 0.07 X_0$ external to the TRT.

Equivalently, Figure 13 shows the total material due to the TRT alone, with and without the TRT services. While the SCT component is important, and should be minimised, the active and passive TRT material is dominant. This material also affects the pattern recognition capability and speed in high-multiplicity environments such as b-jets; the loss of a hit on a track is preferable to the inclusion of a spoiled hit on that track.

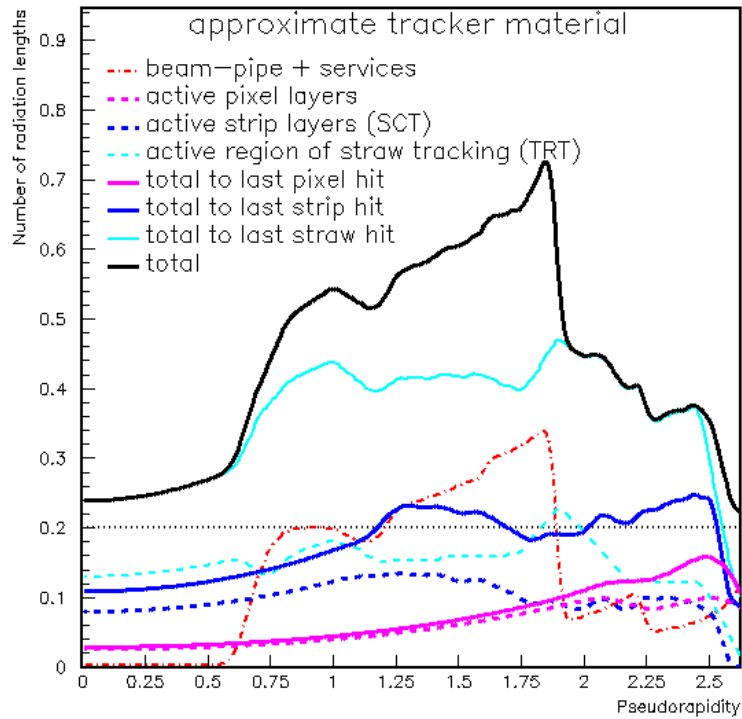


Figure 12: Material distribution after removal of the SCT external services. To be compared with Figure 10.

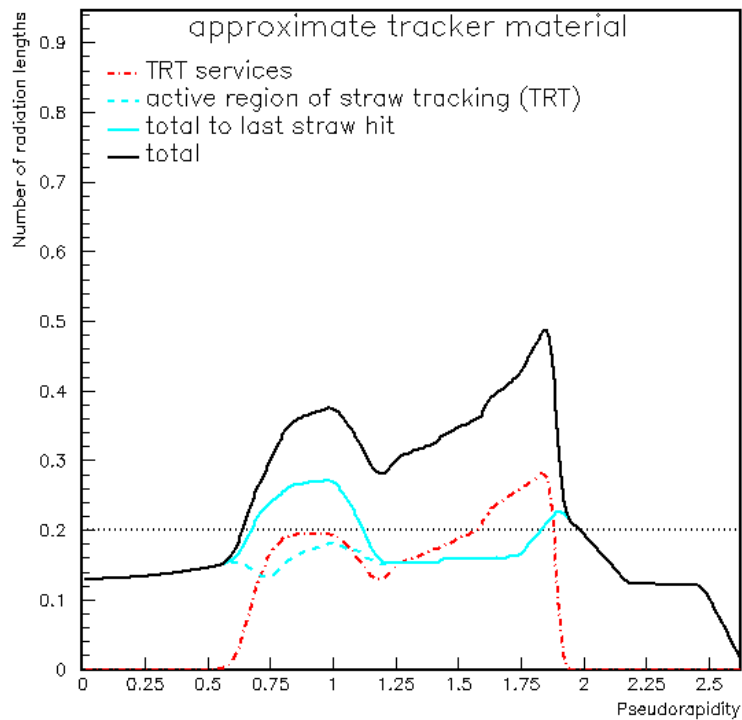


Figure 13: Material distribution for the TRT alone, with and without services.

3.4 A summary of comments relevant to Section 3

Significant savings on the material preceding the TRT have been made by re-routing the pixel services outside the tracking acceptance, that is in the region $|\eta| > 2.5$. A further reduction of material in the active volume of the tracker has resulted from a revised pixel layout. This layout significantly reduces the pixel area, but does require pixel replacement during its operational lifetime.

The following issues are relevant to the suggested service routing and revised layout:

1. The priority of robust high-luminosity tracking with good efficiency in the region $|\eta| < 2.5$, as compared with $|\eta| < 2.0$, should be re-assessed. An optimized tracker design is significantly affected by the requirement of low material in the region $2.0 < |\eta| < 2.5$.
2. The specification of $0.2X_0$ as a maximum material specification preceding the continuous tracking layers, needs further quantitative evaluation.
3. The layout of services in the forward direction should be considered if:
 - relevant services can be demonstrated to be radiation tolerant,
 - physics signals are not significantly deteriorated by a poorer calorimeter,
 - adequate calorimeter resolution is maintained in the extreme forward direction,
 - splash-back from showers outside the tracking acceptance does not create an unacceptable background of false 'in-time' hits in the forward SCT and TRT detectors.
4. Atlas should consider a realistic replacement strategy for Inner Detector elements, including access scenarios. The present Atlas strategy for SCT operation over a 10 year operating lifetime is a substantial constraint on the layout.

Key issues remain:

- the possible reduction of SCT material/support for the current layout,
- whether the SCT layout be improved within existing envelope (4 layers because of pattern recognition),
- the possible reduction of TRT support, cable, radiator and gas material

4.0 Provisional comments relating to the SCT and TRT

Attempts have been made to further reduce the material specification of $0.2X_0$ preceding the TRT by a change to the SCT layout.

It was originally anticipated that significant reductions would be possible using an extended barrel with a smaller number of forward disks. Unfortunately, the angle effect at large rapidity more than negates the effect of a reduced disk area, especially as (unlike the pixels) services must still traverse the tracking acceptance. Studies have included the inclusion of a longer barrel with a reduced number of forward disks.

Alternatively, it is attractive to reduce the barrel radius, but as noted below, for a given barrel length this also results in an increased effective material from the angle effect. More generally, while maintaining the present tracker acceptance and space point specification for the

existing SCT envelope and engineering assumptions, we have not so far achieved a significant further reduction of material.

As one of many examples, Figure 14 shows the layout after replacing the $r=52\text{cm}$ barrel by a barrel of radius $r=22\text{cm}$. One disk has been removed in the forward direction, and the remaining disks have been (approximately) re-aligned. Subject to an Atlas replacement policy, this layout change is attractive. However, because of the angle effect (see Figure 15), the total material preceding the TRT reaches $0.28X_0$. On the other hand, a shorter barrel for the 22cm layer would result in increased service material.

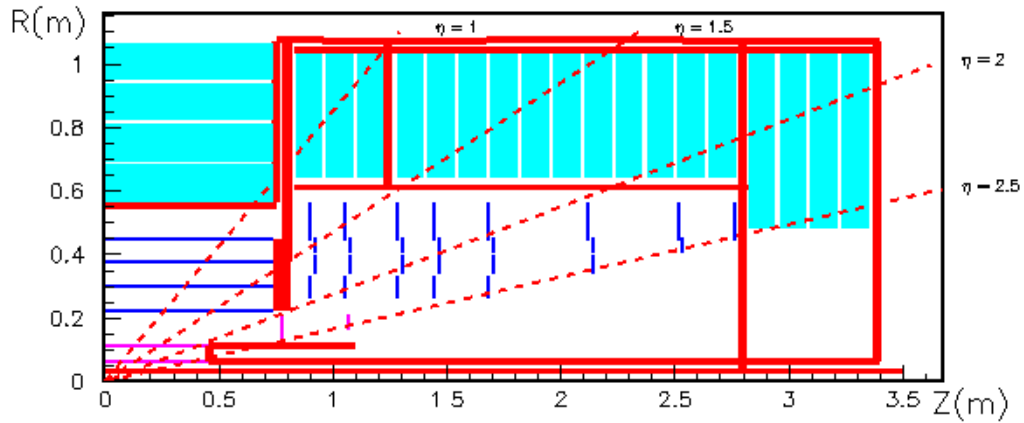


Figure 14: Revised SCT layout.

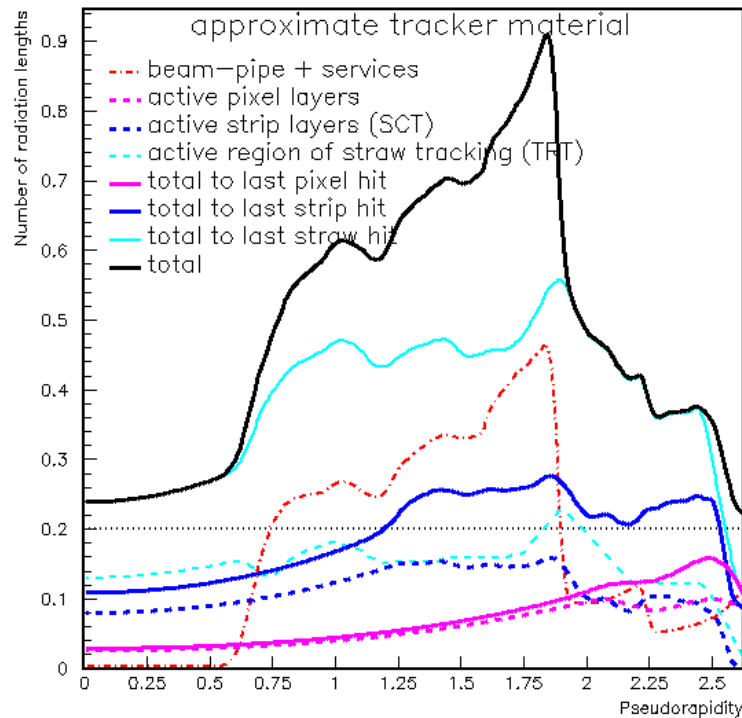


Figure 15: Material distribution for the layout of Figure 14.

Further studies (for example reducing the barrel length for both the SCT and TRT) are in progress.

Finally, as discussed above, Figure 13 shows the total material due to the TRT alone, with and without the TRT services.

Acknowledgement

We wish to thank Trivan Pal for several productive discussions and suggestions. We also thank Jo Pater for explanations on the material as inserted to the DICE Monte Carlo program.

References

1. Presentation to the ATLAS Inner Detector Working Group, INDET-TR-029, T. Pal (September 1996)
2. See also INDET-TR-220, T. Pal (September 1996)
3. Inner Detector note in preparation, D. Froidevaux and J. Pater
4. ATLAS internal note, INDET-NO-046, D. Froidevaux and A. Parker (1994)
5. ATLAS internal note, INDET-NO-127, T. Pal et al. (March 1996)
6. ATLAS internal note, INDET-NO-015, A.G. Clark et al. (1992)
7. Report to the ATLAS Inner Detector Working Group and report to the Inner Detector Steering Group, H. Ogren and A. Roumaniouk (September 1996)
8. Private communication, T. Pal